© The American Society of Gene & Cell Therapy

Inactive ERBB Receptors Cooperate With Reactive Oxygen Species To Suppress Cancer Progression

Matthew R Hart[1], Hsin-Yuan Su[2], Derrick Broka[3], Aarthi Goverdhan[3] and Joyce A Schroeder[1–5]

[1]Program in Genetics, University of Arizona, Tucson, Arizona, USA; [2]Program in Cancer Biology, University of Arizona, Tucson, Arizona, USA; [3]Arizona Cancer Center, University of Arizona, Tucson, Arizona, USA; [4]Department of Molecular and Cellular Biology, University of Arizona, Tucson, Arizona, USA; [5]BIO5 Institute, University of Arizona, Tucson, Arizona, USA

The ERBB receptors are a family of heterodimerization partners capable of driving transformation and metastasis. While the therapeutic targeting of single receptors has proven efficacious, optimal targeting of this receptor family should target all oncogenic members simultaneously. The juxtamembrane domains of ERBB1, ERBB2, and ERBB3 are highly conserved and control various aspects of ERBB-dependent biology. In an effort to block those functions, we have targeted this domain with decoy peptides synthesized in tandem with a cell-penetrating peptide, termed EJ1. Treatment with EJ1 induces cell death, promotes the formation of inactive ERBB multimers, and results in simultaneous reduction of ERBB1, ERBB2, and ERBB3 activation. Treatment also results in the activation of myosin light chain–dependent cell blebbing while inactivating CaMKII signaling, coincident with the induction of cell death. EJ1 also directly translocates to mitochondria, correlating with a loss of mitochondrial membrane potential and production of reactive oxygen species. Finally, treatment of a mouse model of breast cancer with EJ1 results in the inhibition of tumor growth and metastasis without associated toxicities in normal cells. Overall, these data demonstrate that a portion of the ERBB jxm domain, when used as an intracellular decoy, can inhibit tumor growth and metastasis, representing a novel anticancer therapeutic.

Received 6 June 2013; accepted 14 August 2013; advance online publication 1 October 2013. doi:10.1038/mt.2013.196

INTRODUCTION

The misregulation or overexpression of ERBB1 (epidermal growth factor receptor, EGFR), ERBB2 (HER2/Neu), and ERBB3 in numerous solid cancers, including non-small cell lung, pancreatic, and breast cancer, has been correlated with reduced overall survival rate and increased disease recurrence in patients (reviewed in ref. 1). Current therapies targeting this receptor family involve the use of ERBB-specific tyrosine kinase inhibitors and monoclonal antibodies. Although several of these therapies have been approved for use by the US Food and Drug Administration, their clinical efficacy is largely limited to those cancers with receptor amplifications or mutations.[2,3]

A myriad of separate, nontraditional, and/or non-kinase-related functions of the ERBB receptors have been demonstrated in the past 2 decades. These include their ability to translocate to the nucleus and act as transcriptional cofactors, in addition to participating in DNA damage repair and replicative pathways, their involvement in calcium signaling, and their ability to traffic to mitochondria, where they can interact directly with cytochrome c oxidase subunit II to affect cellular adenosine triphosphate (ATP) levels and apoptosis.[4–7] The highly conserved juxtamembrane (jxm) domain of the ERBB receptors, located immediately cytosolically of the transmembrane domain, has been shown to be involved in all of these processes. For example, translocation of ERBB1 to the nucleus involves a tripartite nuclear localization sequence of basic amino acids (amino acids 645–657) within the jxm region, previously shown to facilitate the interaction between ERBB1 and importin β1.[8–10] Nuclear ERBB1 interacts with the promoters of several genes, including cyclin D, b-myb, cyclooxygenase 2 (COX2), inducible nitric oxide synthase (iNOS), and breast cancer resistance protein (BCRP) to upregulate their transcription, effecting proliferation, stress response, and resistance to chemotherapeutics.[7,11] Along with its involvement in nuclear trafficking, this same jxm region is important for ERBB1 trafficking to the mitochondria as its deletion reduces ligand-mediated mitochondrial colocalization.[6] Finally, this region is also involved in basolateral membrane localization and can serve as an autonomous targeting domain.[12]

In addition to these effects on subcellular localization, ERBB jxm domains are integral to receptor dimerization. These domains are partly responsible for both maintaining the inactive conformation of an ERBB monomer through electrostatic interactions with the plasma membrane and facilitating the interaction of two ERBB receptors in an active dimer formation.[13] These interactions of the ERBB jxm can be further modulated by calcium influx. ERBB1-mediated elevation of free Ca^{2+} levels in the cytoplasm induces activation of calmodulin (CaM) and leads to the association of Ca^{2+}/CaM and the ERBB jxm domain, enabling signaling downstream of both the ERBB receptor and Ca^{2+}/CaM, including the activation of CaM-dependent kinase II (CaMKII) and myosin light chain kinase (MLCK).[14–16] Similar functions, including dimerization, nuclear translocation, and calcium signaling, have been shown for this highly homologous jxm region in other ERBB family members.[9,17–20]

The first two authors contributed equally.

Correspondence: *Joyce A. Schroeder, Arizona Cancer Center 1515 N Campbell Ave, Tucson, AZ 85724, USA. E-mail: joyces@email.arizona.edu*

© The American Society of Gene & Cell Therapy

In this study, peptides were created to represent subdomains within ERBB1, from amino acids 643–663, and were tested for their ability to affect cell survival. We demonstrate the ability of one of these jxm peptides to enter and kill cancer cells; regulate ERBB multimerization and activation; and regulate both calcium and mitochondrial pathways of cell survival. We also show that in a mouse model of breast cancer, treatment with this peptide displays no observable toxicity and has the ability to reduce tumor growth and metastasis.

RESULTS

ERBB1 jxm peptides reduce cellular viability

The conserved jxm domains of ERBB1, ERBB2, and ERBB3 contain sequences responsible for receptor dimerization, CaM binding, nuclear and mitochondrial localization, and membrane targeting (**Figure 1a**,**b**).[9,12,17–23] Therefore, we set out to determine whether blocking the function of the jxm domain of the ERBB receptors would result in an effective ERBB-dependent cancer therapeutic strategy. To do this, we created cell-penetrating peptides to act as dominant-negative "decoys," thereby inhibiting endogenous jxm interactions. Peptides specific for jxm subdomains were synthesized downstream of the protein transduction domain-4 (PTD4;[24] **Figure 1c**). Next, the effect of peptide treatment on cell viability was analyzed on the breast cancer cell line MDA-MB-468 by MTT (3-[4,5-dimethylthiazol-2-y1]-2,5-diphenyl tetra-zolium bromide) analysis after 3 days of treatment. We found that the amino acid region between hERBB1$^{643–663}$ (EJ1) demonstrated optimal reduction in viability, and partial reduction was also obtained with subsequences within EJ1, including EJ2 (hERBB1$^{643–655}$), EJ3 (hERBB1$^{649–663}$), and EJ5 (hERBB1$^{653–663}$; **Figure 1c**,**d**).

To test the role of charge of the peptide, one of the basic amino acids (Arg or Lys) in each of the three basic clusters of EJ1 was substituted with an acidic amino acid (Asp; EJ10, hereafter referred to as the control peptide, CP), and this step completely ablated the effects on viability (**Figure 1c**,**d**). Substituting those same basic amino acids with polar amino acids (Gln; EJ11) instead only marginally blocked the antiproliferative effects of EJ1 (**Figure 1d**). Note that replacement of the eight arginines and lysines with alanines resulted in an insoluble peptide (EJ8). Together, these results strongly implicate charge in the function of EJ1.

To determine whether the minimal nuclear localization sequence (EJ4) or the minimal basolateral domain (EJ6) was responsible for the antiproliferative effects of EJ1, peptides of these subdomains were created. No antiproliferative effect was observed for either peptide, implicating the CaM-binding and dimerization domains as essential for cell death (**Figure 1a**,**c**,**d**). After determining the optimal peptide concentration (20 μmol/l; **Figure 1e**), EJ1 was tested for its ability to affect cell viability in additional breast cancer cell lines including T47D (**Figure 1f**) and MDA-MB-231 (**Figure 1g**), the immortalized breast epithelial cell line MCF10A (**Figure 1h**), and pancreatic cancer cell lines including BxPC3 (**Figure 1i**), AsPC1 (**Figure 1j**), and MIA PaCa-2 (**Supplementary Figure S1c**). In analyzing the effects of EJ1 in these lines, we found that its effects on cellular viability ranged from a minimum reduction of 1% in MIA PaCa-2 cells and 10% in AsPC1 (**Figure 1j**) and MDA-MB-231 cells (**Figure 1g**) to a maximum of 60% reduction in T47D cells during a 3-day treatment period (**Figure 1f**). Analysis of the ERBB expression profile (including ERBB1, ERBB2, and ERBB3) in these cell lines demonstrated expression of at least two out of the three ERBB receptors in each of the lines (**Supplementary Figure S1a**). Interestingly, AsPC1, MIA PaCa-2, and 231 cells, all of which showed little response to EJ1 treatment, possess mutant forms of the protein Kras. Importantly, EJ1 had no effect on the viability of immortalized Chinese hamster ovary (CHO) cells that express low endogenous levels of the ERBB receptors (**Supplementary Figure S1b**).

EJ1 inhibits ERBB activation while promoting receptor multimerization

To determine whether EJ1 affects ERBB1 activity, we first treated both MDA-MB-468 (**Figure 2a**) and BxPC3 cells (**Supplementary Figure S2**) with EJ1, CP, or vehicle in the presence or absence of EGF to activate ERBB1. We found that EJ1 significantly suppressed EGF-induced phosphorylation of ERBB1. This suppression also affected downstream signaling partners, resulting in a reduction of p-AKT (**Figure 2a**). Interestingly, treatment with EJ1 also resulted in a loss of total protein for AKT and p38 (**Figure 2a**). In addition, an increase of the activated stress response kinase, p38, was observed after EJ1 treatment.

In addition to blocking the activation of ERBB1, we found that EJ1 treatment similarly inhibited the *trans*-phosphorylation of ERBB2 and ERBB3 in response to EGF (**Figure 2b**,**c**). Note that BxPC3 cells were used to test ERBB2 activation because 468 cells do not express detectable levels of ERBB2. Because EJ1 peptide mimics the dimerization domain of ERBB1, a domain that is conserved in ERBB2 and ERBB3 (**Figure 1a**,(**B**)), we next evaluated the ability of EJ1 to block dimerization. To first evaluate the effects of EJ1 on ERBB1 homodimers, MDA-MB-468 cells were treated with EGF in addition to EJ1 or controls in the presence of a nonreducible cross-linker. Surprisingly, we found that EJ1 induced the formation of high-molecular-weight ERBB1 multimers (**Figure 2d**, arrow). To determine whether EJ1 had a similar effect on heterodimer formation, cells were treated with EGF in the presence of EJ1 or controls and evaluated for the formation of ERBB1/ERBB3 heterodimers by co-immunoprecipitation. Again, EJ1 treatment resulted in suppression of ERBB3 phosphorylation and an increase in the formation of ERBB1/ERBB3 heterodimers even in the absence of serum (**Figure 2e**). Finally, we observed a direct interaction between ERBB1 and EJ1 by the pull down of biotinylated EJ1 with ERBB1, which preferentially occurred in the absence of EGF treatment (**Supplementary Figure S3**). Together, these results indicate that EJ1 interacts with ERBB1 and promotes the inactive multimerization of ERBB receptors.

EJ1 affects Ca^{2+}/CaM downstream signaling

In addition to the dimerization domain, the sequence for EJ1 overlaps with the CaM-binding domain for ERBB1.[25] Ca^{2+}/CaM signaling regulates many different cellular events, such as membrane dynamics, cell survival, mitochondrial function, and motility (reviewed in refs 26,27). We began by evaluating whether EJ1 was affecting membrane dynamics by treating MDA-MB-468 cells with either CP (**Figure 3a** (A–D)) or EJ1 (**Figure 3a** (E–H)) and examining cell morphology. We found that in 15 minutes, EJ1-treated cells formed large membrane protrusions or blebs (**Figure 3a**

© The American Society of Gene & Cell Therapy

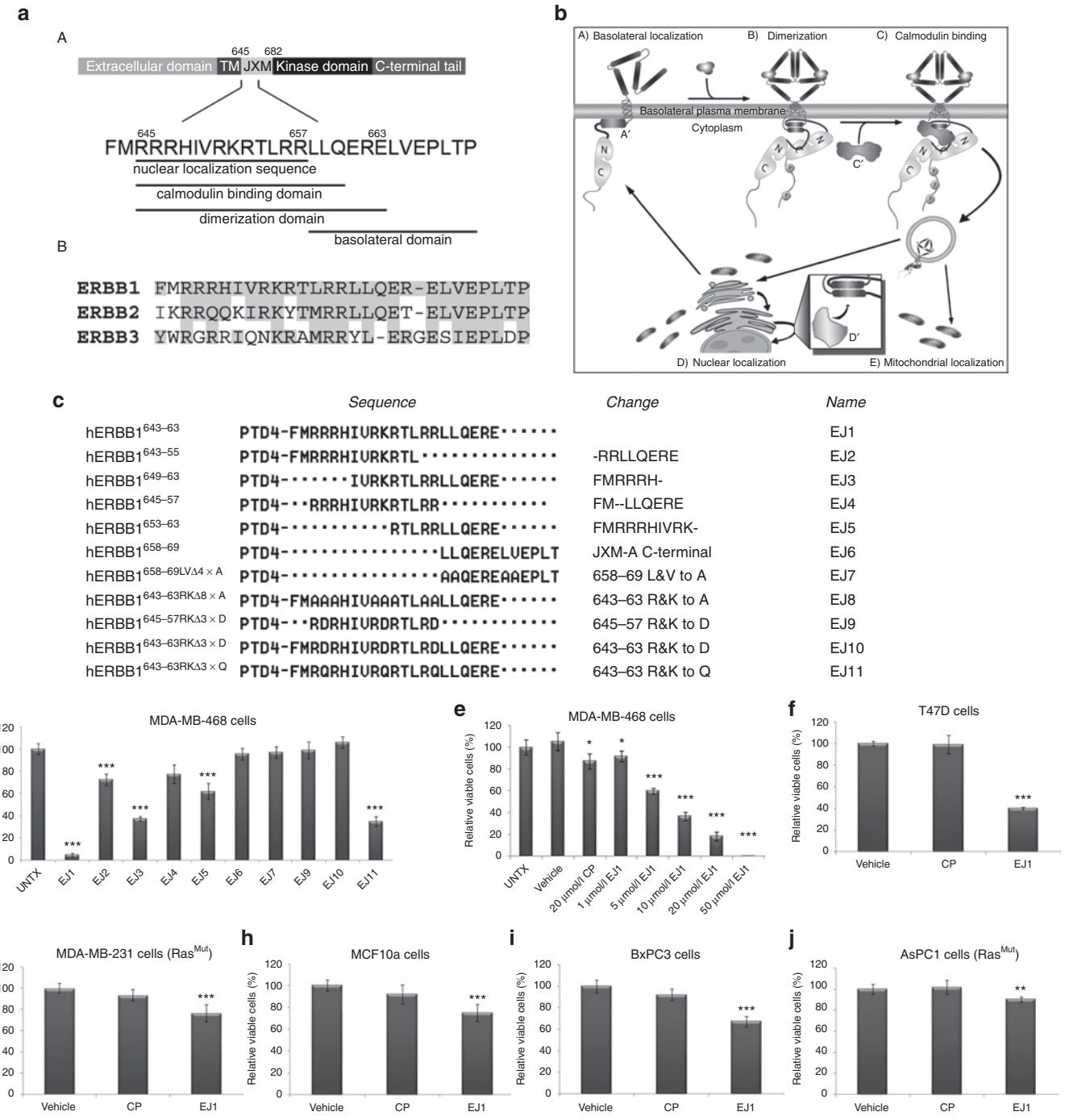

Figure 1 Juxtamembrane domain peptides reduce cell viability. (**a**) (A) Schematic diagram depicting relevant functional motifs of the ERBB1 juxtamembrane (jxm) domain and (B) jxm domains of ERBB1, ERBB2, and ERBB3, with conserved regions based on National Center for Biotechnology Information protein alignment highlighted in gray. (**b**) Model of interactions involving the ERBB1 jxm. (A) ERBB1 localizes through its jxm (A′)-contained targeting domain to the basolateral plasma membrane. (B) Ligand binding induces conformational changes in ERBB1, whereby interactions between jxm$^{645–663}$ and the plasma membrane are disrupted, allowing dimerization and *trans*-phosphorylation. (C) Ca^{2+} influx promotes ERBB1 jxm domain interactions with proteins such as calcium-bound calmodulin (Ca^{2+}/CaM) (C′). (D) Internalization and association with proteins such as importins α/β (D′) and trafficking to locations such as the nucleus and mitochondria (D, E). (**c**) The amino acid number of ERBB1 is shown in the left column, corresponding to the specific amino acids shown in the middle column (sequence). Peptide designations are indicated in the right column. Changes from EJ1 in EJ2–11 are denoted in the second column from the right. (**d–j**) Cell lines were treated daily with 20 μmol/l EJ1, 20 μmol/l CP, or vehicle (water) for 3 days unless otherwise noted, and cell viability was determined by the MTT assay. Growth rates for vehicle-treated cells were set to 100%, and CP and EJ1 rates were adjusted accordingly. *$P < 0.05$, **$P < 0.01$, ***$P < 0.001$ (Student's *t*-test). Error bars, mean ± SD.

(F, arrows)). By 60 minutes of treatment, cells had formed large intracellular vacuoles (**Figure 3a** (G, arrowheads)). After 16 hours, many EJ1-treated cells appeared dead (**Figure 3a** (H)). In an effort to determine whether the cell blebbing corresponded to ERBB1 localization, cells were treated with Texas-Red-labeled EGF, Alexa Fluor 488–labeled transferrin, and EJ1 simultaneously (**Figure 3b**

© The American Society of Gene & Cell Therapy

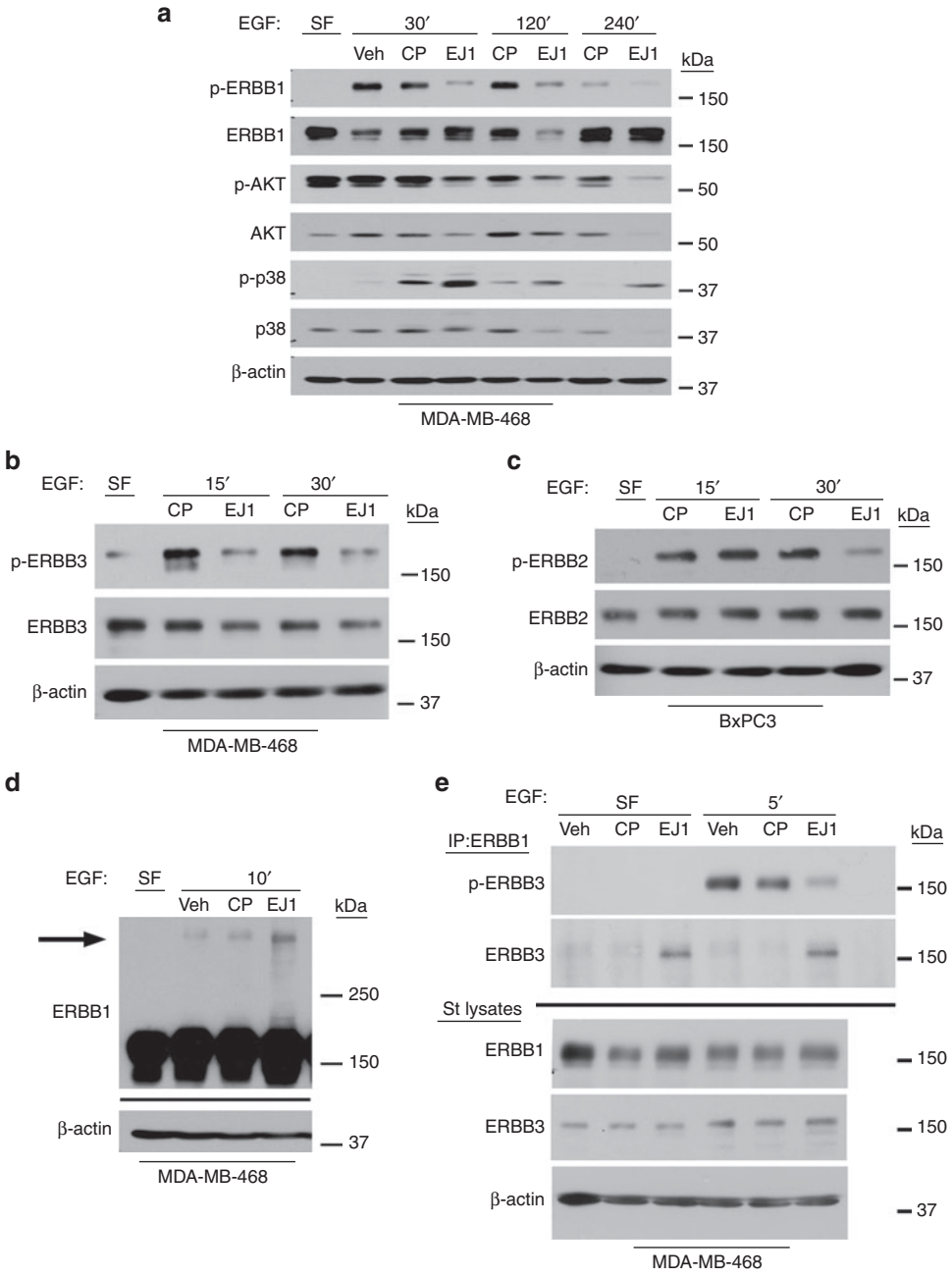

Figure 2 EJ1 peptide induces the formation of inactive ERBB multimers. (**a, c**) MDA-MB-468 cells or (**b**) BxPC3 cells were treated with 100 or 50 ng/ml EGF (respectively) in combination with water (Veh), 20 μmol/l CP, or 20 μmol/l EJ1 for the indicated times and lysed. Protein levels were determined as indicated. (**d**) MDA-MB-468 cells were treated with peptides for 10 minutes on ice. Then, 100 ng/ml EGF was added to the medium and incubated for another 10 minutes on ice, followed by cross-linking with 3 μmol/l DMS. Lysates were evaluated by western blotting for ERBB1 and β-actin. (**e**) MDA-MB-468 cells were treated similarly, but without cross-linker, lysed, and immunoprecipitated (ERBB1 Ab-13). Molecular weights are shown to the right.

and **Supplementary Figure S4**). Although both ligands were detected in cells treated with EJ1, large membrane protrusions quickly formed specifically where EGF was concentrated, resulting in focused membrane explosions (**Figure 3b** (F-F', arrowhead) and **Supplementary Figure S4** (arrowheads)]. This indicates that EJ1-induced membrane blebbing occurs in membrane regions containing ERBB1. To investigate whether membrane blebbing is a result of ERBB1 kinase inhibition, MDA-MB-468 cells were treated with AG1478, an ERBB1 kinase inhibitor, and membrane dynamics were observed (**Supplementary Figure S5**). No membrane blebbing was observed, indicating that membrane blebbing is not a result of kinase inhibition.

Ca^{2+}/CaM signaling regulates many different downstream pathways, such as CaMKII and MLCK. CaMKII regulates cell proliferation, whereas MLCK phosphorylates myosin light chain (MLC) and regulates actinomyosin reorganization during membrane blebbing (as depicted in **Figure 3c**). To investigate whether EJ1-induced membrane blebbing was through the MLCK

© The American Society of Gene & Cell Therapy

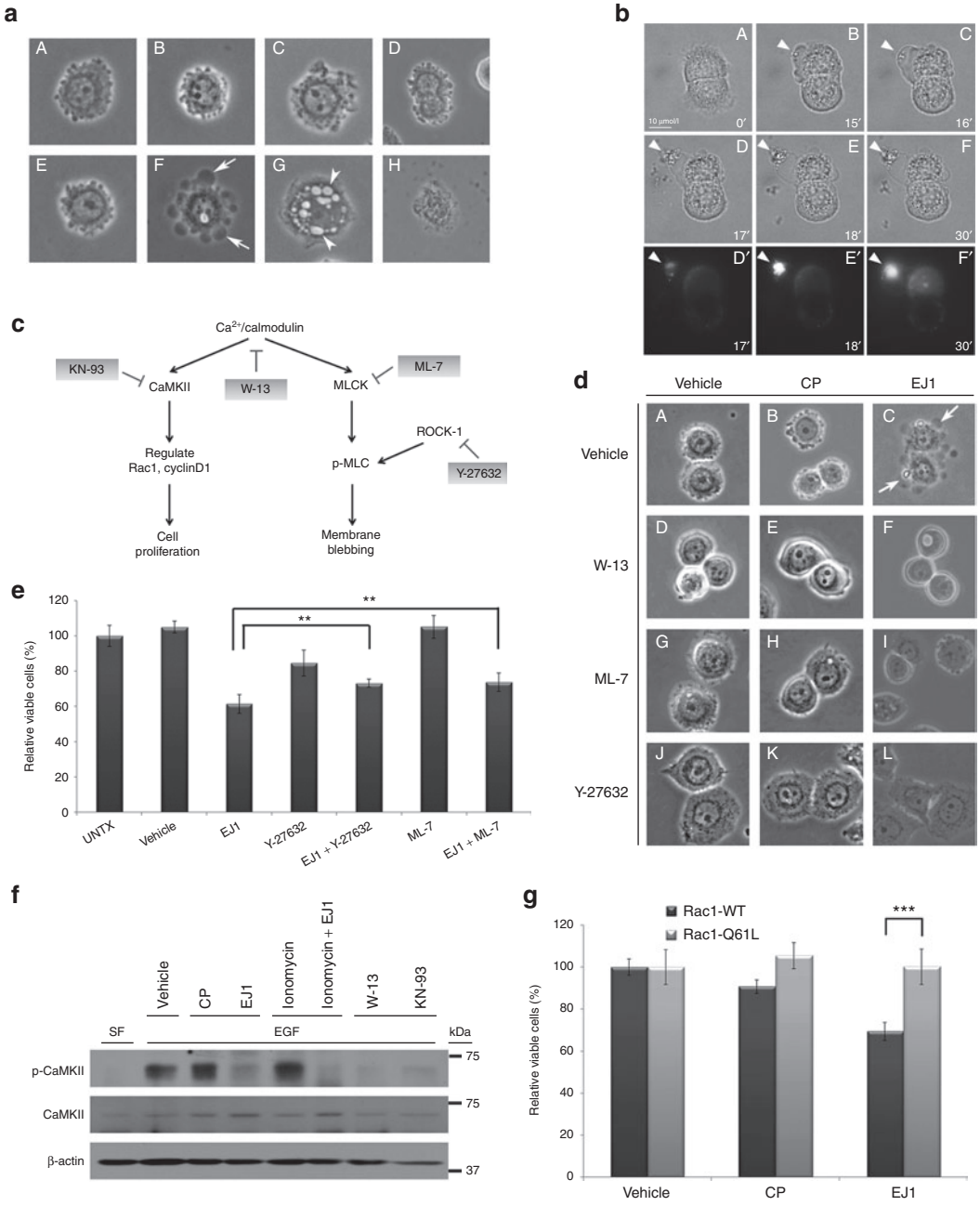

Figure 3 EJ1 peptide affects Ca^{2+}/CaM downstream signaling. (**a**) MDA-MB-468 cells were treated with either 20 μmol/l CP (A–D) or 20 μmol/l EJ1 (E–H) for 0 minutes (A, E), 15 minutes (B, F), 60 minutes (C, G), or 16 hours (D, H). Arrows indicate membrane blebs and arrowheads indicate intracellular vacuoles. (**b**) BxPC3 cells were serum starved overnight, then treated with 20 μmol/l EJ1 and 50 ng/ml Texas-Red-labeled EGF, and imaged for 30 minutes with an Olympus IX71 deconvolution microscope. Panels A–F are bright field images, D′–F′ are red channel images (Texas-Red-labeled EGF). Arrowheads indicate locations of EGF accumulation on membrane protrusions (see also **Supplementary Figure S4**). (**c**) Diagram depicts Ca^{2+}/CaM-regulated signaling pathway, and inhibitors acting at different targets are indicated. (**d**) MDA-MB-468 cells were pretreated with 50 μmol/l W-13 (D–F), 10 μmol/l ML-7 (G–I), or 10 μmol/l Y-27632 (J–L) in complete medium at 37 °C for 30 minutes and then treated with vehicle, 20 μmol/l CP, or 20 μmol/l EJ1 in combination with W-13, ML-7, or Y-27632 in complete medium at 37 °C for 15 minutes. Images represent the bright field images. Arrows indicate membrane blebbing. (**e**) MDA-MB-468 cells were untreated (UNTX) or treated with water (Vehicle), 20 μmol/l EJ1, 10 μmol/l Y-27632, or 10 μmol/l ML-7 alone or EJ1 in combination with Y-27632 or ML-7, and the viability was assessed by the MTT assay. $^{**}P < 0.01$ (Student's *t*-test). Error bars, mean ± SD. (**f**) MDA-MB-468 cells were either in serum-free medium (SF) or stimulated with 100 ng/ml EGF (EGF) and then incubated with water (Vehicle), 20 μmol/l CP, 20 μmol/l EJ1, 2 μmol/l ionomycin, 50 μmol/l W-13, 100 μmol/l KN-93, or EJ1 in combination with ionomycin for 15 minutes. Lysates were immunoblotted with antibodies as indicated. (**g**) Stable, neomycin-selected NIH3T3 cell lines were created, expressing either Rac1 wild-type (Rac1-WT) or Rac1 constitutively active mutant (Rac1-Q61L). Cells were treated with water (Vehicle), 20 μmol/l CP, or 20 μmol/l EJ1, and the viability was assessed by MTT. $^{***}P < 0.001$ (Student's *t*-test). Error bars, mean ± SD.

© The American Society of Gene & Cell Therapy

pathway, MDA-MB-468 cells were treated with vehicle, CP, or EJ1 alone (**Figure 3d** (A–C)] or in combination with the CaM inhibitor W-13 or the MLC phosphorylation inhibitors ML-7 and Y-27632 (**Figure 3d** (D–L)). We found that both the CaM inhibitor W-13 and the MLC phosphorylation inhibitors ML-7 and Y-27632 completely inhibited EJ1-induced membrane blebbing (**Figure 3d**). To determine whether these effects on membrane blebbing were related to cell survival, the inhibitors were used in conjunction with EJ1 in an MTT assay. We observed that after 1 day of treatment, both Y-27632 and ML-7 could significantly reduce the effects of EJ1 (**Figure 3e**).

To determine whether EJ1 could also affect CaMKII activation, MDA-MB-468 cells were treated with vehicle, CP, or EJ1 with or without ionomycin, an ionophore capable of inducing Ca^{2+}/CaM signaling (**Figure 3f**). Although EGF and ionomycin both induced CaMKII phosphorylation, this induction was suppressed by EJ1. To test whether inhibition of CaMKII activity was one of the causes of cell death, we used NIH3T3 cells overexpressing Rac1, one of the key downstream effectors of CaMKII, and assessed cell viability in response to EJ1 (**Figure 3g**). Overexpression of constitutively active Rac1 (Rac1-Q61L), compared with wild-type Rac1 (Rac1-WT), significantly rescued EJ1-induced cell death (**Figure 3g**). These results indicated that suppression of CaMKII activation by EJ1 could be circumvented by overexpression of an activated downstream component of the CaMKII pathway. Taken together, EJ1 can simultaneously activate the MLCK pathway and inhibit the CaMKII pathway, and both pathways are integral to the EJ1-mediated reduction in cell survival.

EJ1 affects cell survival through apoptosis/necrosis

To investigate the vacuoles formed in **Figure 3a** further, we performed transmission electron microscopy (**Figure 4a**). MDA-MB-468 cells were treated with EJ1 and evaluated at several time points (**Figure 4 a** (A–D)). By 30 minutes, double-membrane structures (**Figure 4a** (C', arrowheads)) filled with organelle debris (**Figure 4a** (C', filled arrows)) and electron-dense deposits

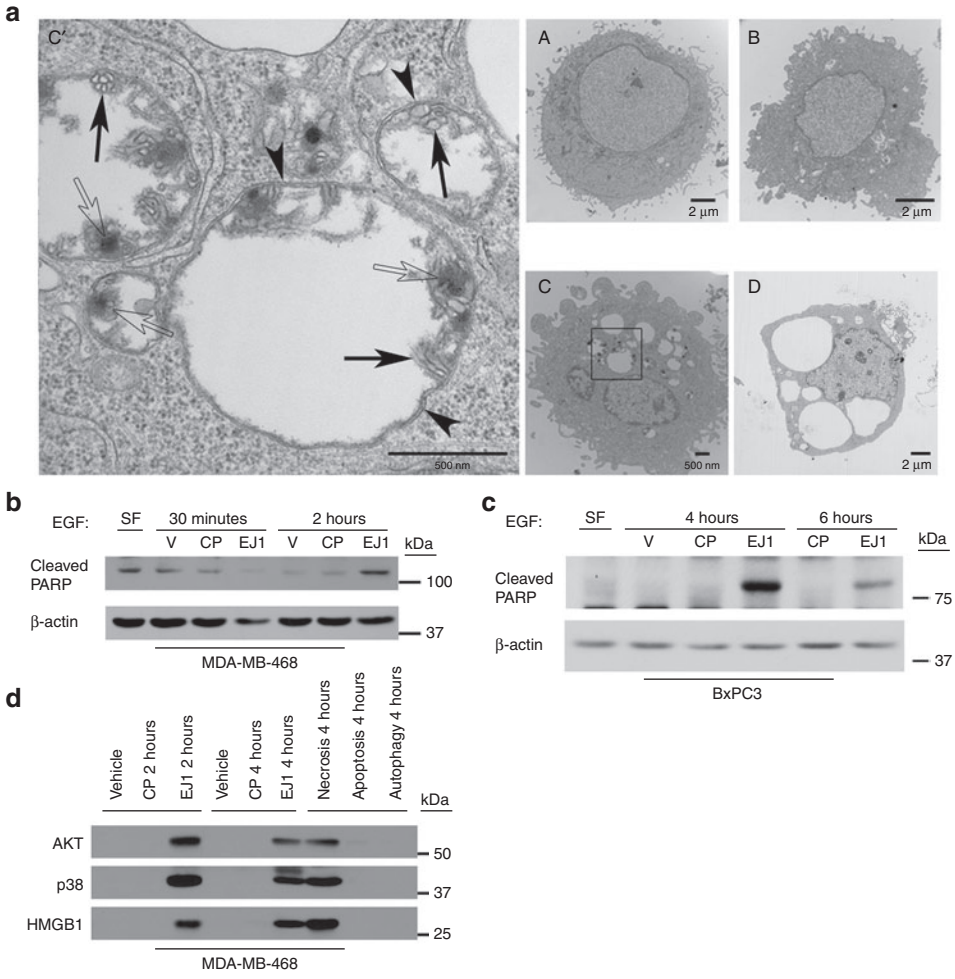

Figure 4 EJ1 peptide induces both apoptosis and necrosis. (**a**) MDA-MB-468 cells were treated with 20 µmol/l EJ1 for (A) 0 minutes, (B) 5 minutes, (C and C') 30 minutes, or (D) 2 hours and then prepared for transmission electron microscopy (TEM). Arrowheads indicate double membrane structures, filled arrows indicate organelle debris, and open arrows indicate electron-dense deposits. (**b, c**) MDA-MB-468 and BxPC3 cells were serum starved before treatment with EGF at 100 or 50 ng/ml respectively, along with water (V), 20 µmol/l CP, and 20 µmol/l EJ1 for indicated time points and lysed. (**d**) MDA-MB-468 cells were treated as in (**b**) along with 10 ng/ml human TNF-α and 35 µmol/l cycloheximide (apoptosis inducer), 2 µmol/l ionomycin and 50 µmol/l CCCP (necrosis inducer), and 100 nmol/l rapamycin (autophagy inducer) for the indicated times and media were collected. Protein in medium was precipitated as described in ref. 28.

© The American Society of Gene & Cell Therapy

(**Figure 4a** (C', open arrows)) were observed in EJ1-treated but not untreated cells (**Figure 4a** (A)). As double-membrane structures are hallmarks of autophagy and membrane blebbing is a hallmark of apoptosis, we next evaluated the cells for induction of each of these events. Evaluation of the conversion of microtubule-associated protein 1 light chain 3-I or II upon treatment with EJ1 indicated that the peptide was inducing some level of autophagy (**Supplementary Figure S6a**). However, the autophagy inhibitor, 3-MA, was not able to rescue EJ1-induced effects on cell viability, membrane morphology, or vacuole formation, suggesting that any induced autophagy was more likely a protective response to EJ1 rather than a mode of cell death (**Supplementary Figure S6b,c**).

To investigate whether the cell death was apoptosis related, MDA-MB-468 and BxPC3 cells were evaluated for PARP cleavage (**Figure 4b,c**) with a strong induction observed upon EJ1 treatment compared with CP treatment at 2, 4, and 6 hours, indicating an induction of apoptosis by EJ1. Further analysis of apoptosis by propidium iodide and Annexin V staining with flow cytometry at 4 hours also revealed an EJ1-induced increase in the percentage of Annexin V–positive cells compared with treatment with CP (**Supplementary Figure S7**). This induction was particularly strong in BxPC3 cells under serum-free conditions. To evaluate necrosis as an additional factor in cell death, culture media from EJ1-treated MDA-MB-468 cells was collected and evaluated for the release of the nuclear protein HMGB1.[28] We found detectable HMGB1 in EJ1-treated but not control-treated cell media (**Figure 4d**). Interestingly, we also found AKT and p38 in EJ1-treated cell media (**Figure 4d**), which was consistent with our previous findings (**Figure 2a**) that EJ1 resulted in loss of cellular AKT and p38. These data indicate that EJ1 causes cell death through both apoptosis and necrosis.

Accumulation of EJ1 at mitochondria causes mitochondrial disruption and reactive oxygen species generation

During our evaluation of intracellular vesicles created by EJ1 treatment, we observed the presence of what appeared to be remnant mitochondrial cristae within these vacuolar structures (**Supplementary Figure S8**). To further explore the effects of EJ1 treatment on mitochondria, MDA-MB-468 cells were labeled with Mitotracker, treated with either EJ1 or CP, and imaged (**Figure 5a** (A–D)). Mitochondria appeared enlarged and rounded very rapidly upon EJ1 treatment (**Figure 5a** (D', arrowheads)). Similar results were observed for T47D, NIH-3T3, CHO, and BxPC3 cells (**Supplementary Figure S9**). To determine whether the mitochondrial membrane was being damaged during this process, cells were treated with JC-1 dye, a reporter of mitochondrial membrane potential (MMP). MDA-MB-468 cells were labeled with JC-1 for 15 minutes and then treated for 2 hours with CP, EJ1, or carbonyl cyanide 3-chlorophenylhydrazone (CCCP), a compound that disrupts mitochondrial integrity, as a positive control for mitochondrial damage. A significant loss of MMP was observed with EJ1 treatment (**Figure 5b**). To determine whether these effects could be due to EJ1 directly interacting with mitochondria, MDA-MB-468 (**Supplementary Figure S10**) and T47D (**Figure 5c**) cells were treated with fluorescein isothiocyanate (FITC)-labeled EJ1 and Mitotracker. Visualization over time demonstrated increased colocalization between EJ1 and mitochondria, indicating that these effects of EJ1 could be due to direct targeting of the mitochondria (**Figure 5c** (A–F, arrows)]. Overall, these results indicate that EJ1 interacts with mitochondrial membranes and causes mitochondrial swelling and loss of MMP.

There are multiple intracellular events that can lead to or result from loss of MMP, such as modulation of Ca^{2+} concentration or reactive oxygen species (ROS) within the cells.[29] To measure intracellular ROS levels in response to EJ1, we used 2′,7′-dichlorofluorescein (DCFH) diacetate, which becomes fluorescent DCF in the presence of ROS. MDA-MB-468 cells were treated with CP, *N*-acetyl cysteine (NAC, a ROS scavenger that reduces intracellular ROS levels), EJ1, or NAC + EJ1 (**Figure 5d** and **Supplementary Figure S11**). While EJ1 treatment increased intracellular ROS levels as indicated by DCF fluorescence, cotreatment with NAC significantly reduced EJ1-induced ROS levels. We next sought to determine whether mitigation of ROS would prevent EJ1-induced cell death. We found that cotreatment of cells with EJ1 and NAC could indeed significantly rescue EJ1-induced cell death (**Figure 5e**). These data demonstrate a role for intracellular ROS in EJ1-mediated cell death.

EJ1 reduces tumor growth and metastasis in MMTV-pyMT transgenic mice

We next set out to determine whether EJ1 would function as an antitumor therapy agent *in vivo*. We tested the peptide on the MMTV-pyMT murine model of breast cancer, which develops synchronous, multifocal mammary tumors in all 10 mammary glands with a multistep progression that resembles human disease.[30,31] Intraperitoneal delivery of several EJ1 dosages were tested, and 20 μg/g body weight was chosen for further study (**Figure 6a**). This dosage of EJ1 ($n = 8$), CP ($n = 5$), or an equivalent volume of PBS ($n = 7$) were then given to tumor-bearing mice, daily, for the course of the study (see "Materials and Methods"). Similar day 0 occupancy and time of treatment are demonstrated for EJ1 and Control mice (**Supplementary Figure S12**). We found that individual tumor growth rates and average tumor size were significantly reduced by treatment with EJ1 compared with CP or PBS (**Figure 6b,c**). Additionally, many resected EJ1-treated tumors were necrotic in appearance compared with those in controls (**Figure 6b** (insets)). Transmission electron microscopy analysis of tumors after treatment also revealed damaged mitochondria in EJ1-treated tumors, similar to those seen *in vitro* (**Figure 6d**). Importantly, no toxicity from this dose of EJ1 was observed (weight loss, grooming behavior, or gross changes to organs upon necropsy). Evaluation of post-study tumor lysates and quantification by densitometry revealed a 10% decrease in ERBB1 expression in EJ1-treated mice, indicating ERBB1-expressing cells may have been selectively targeted. In addition, we observed a 50–60% decrease in doubly phosphorylated form of MAPK/Erk (dpERK) and ~30% increase in the presence of the apoptotic indicator, cleaved PARP, in EJ1-treated mice (**Figure 6f** and **Supplementary Figure S13**). Similar examination of ERBB2 protein and phosphorylation revealed no significant reductions in EJ1-treated animals (**Supplementary Figure S14**).

Our analysis of protein expression in ERBB-related downstream signaling pathways revealed a significant decrease in the

© The American Society of Gene & Cell Therapy

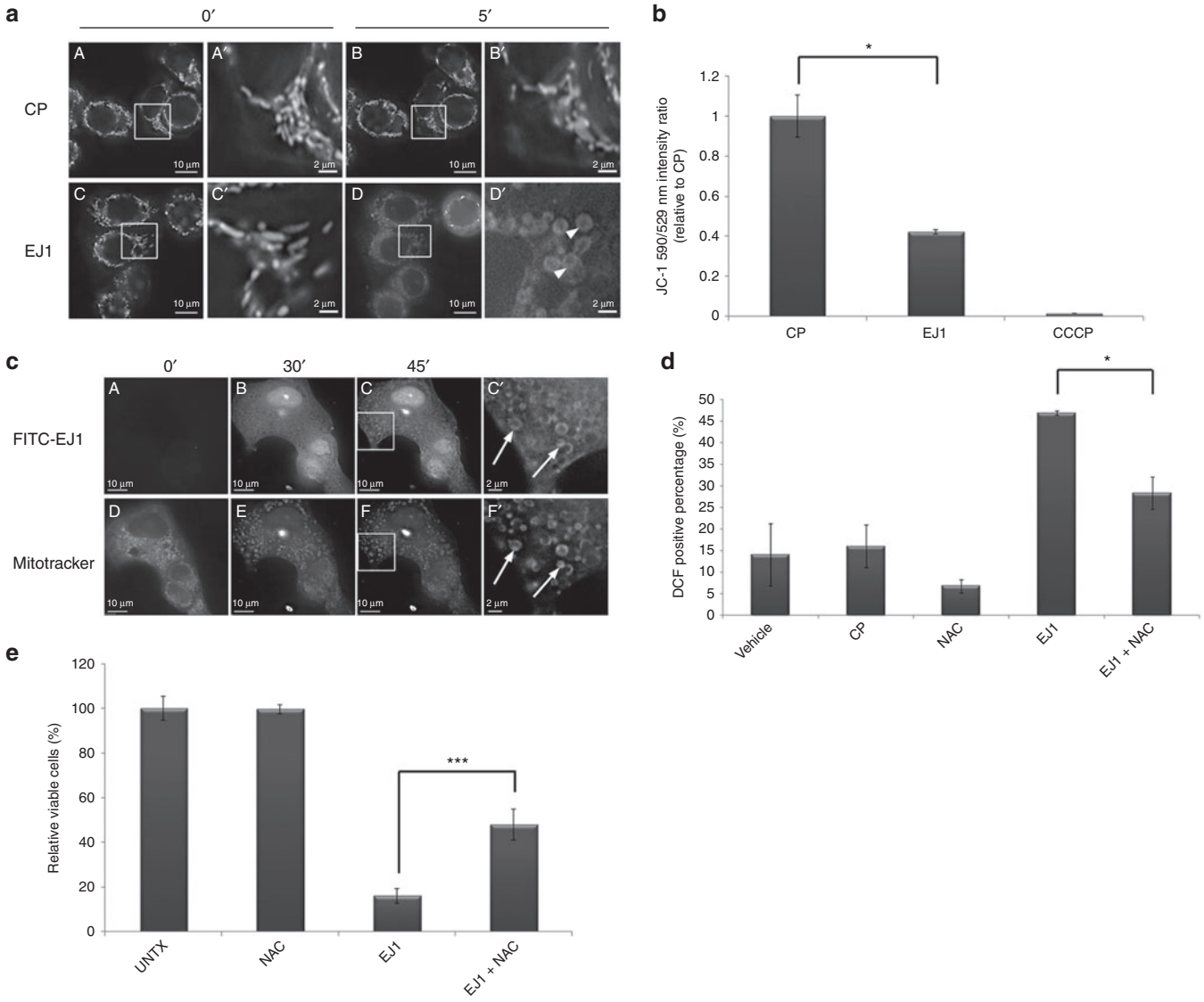

Figure 5 EJ1 peptide localizes to the mitochondria and causes mitochondrial disruption and ROS generation. (**a**) MDA-MB-468 cells were incubated in serum-free media with 200 nmol/l MitoTracker Red CMXRos and 5 μg/ml Hoechst 33342 nuclear stain, followed by either 20 μmol/l CP (A–B′) or 20 μmol/l EJ1 (C–D′), and imaged at 0 minutes (A, A′; and C, C′) or at 5 minutes (B, B′; and D, D′). (**b**) MDA-MB-468 cells were incubated with 1 μmol/l JC-1, followed by 20 μmol/l CP, 20 μmol/l EJ1, or 50 μmol/l CCCP. Results were calculated as the ratio of the 514/590 nm to 514/529 nm fluorescences and the ratio for CP-treated sample was set as 1. *$P < 0.05$, Student's *t*-test. Error bars, mean ± SD. (**c**) T47D cells were treated with MitoTracker (shown in D–F and F′) and Hoechst 33342 as in (**a**) and incubated with 20 μmol/l FITC-labeled EJ1 (shown in A–C and C′). (**d**) MDA-MB-468 cells were stained with 10 μmol/l DCFH-DA, followed by water (Vehicle), 20 μmol/l CP, 0.5 mmol/l NAC, and 20 μmol/l EJ1 or EJ1 in combination with NAC. Cells were then sorted by flow cytometer and analyzed by Cellquest Pro 4.0 software. The results are expressed as the percentage of DCFH fluorescence–positive cells. *$P < 0.05$, Student's *t*-test. Error bars, mean ± SD. (**e**) MDA-MB-468 cells were treated with 0.5 mmol/l NAC alone, 20 μmol/l EJ1 alone, or NAC in combination with EJ1, and viability was assayed by the MTT assay. ***$P < 0.001$, Student's *t*-test. Error bars, mean ± SD.

expression of an ~80-kDa fragment of E-cadherin in EJ1-treated, relative to CP-treated mice (**Figure 6f**, arrow and **Supplementary Figure S13**). Several studies have correlated the expression of the soluble 80-kDa form of E-cadherin with ERBB activity, along with the presence of metastasis or an increased metastatic potential.[32,33] The MMTV-pyMT transgenic mice present with lung metastasis; we therefore evaluated the effects of EJ1 on lung metastasis. Assessment by bright field microscopic analysis and hematoxylin and eosin stain of tissue architecture showed that, on average, the lungs of EJ1-treated mice had significantly less metastatic foci than did comparable Control-treated mice (**Figure 6e** and inset; average controls = 36 metastases/lung, average EJ1 = 12 metastases/lung).

DISCUSSION

In recent years, the essential regulatory role of the jxm domain of the ERBB receptors has been realized (reviewed in ref. 34). In this study, we set out to determine whether this domain could be targeted as an ERBB-dependent anticancer therapeutic strategy. We found that a peptide composed of a 21-amino acid portion of the jxm domain could effectively kill cancer cell lines. We discovered that this

© The American Society of Gene & Cell Therapy

peptide (EJ1) promotes the formation of inactive ERBB dimers and suppresses CaMKII signaling while MLCK-dependent membrane blebbing is promoted, both of which are pathways downstream of a CaM/ERBB interaction. The results of this selective signaling were membrane blebbing and cell death. In addition, EJ1 can affect MMP, involving the generation of ROS and induction of apoptosis/necrosis. Finally, these effects appear to be tumor specific because injection of EJ1 into an immune-competent transgenic mouse model of breast cancer resulted in an inhibition of tumor growth and metastasis without any gross toxicity.

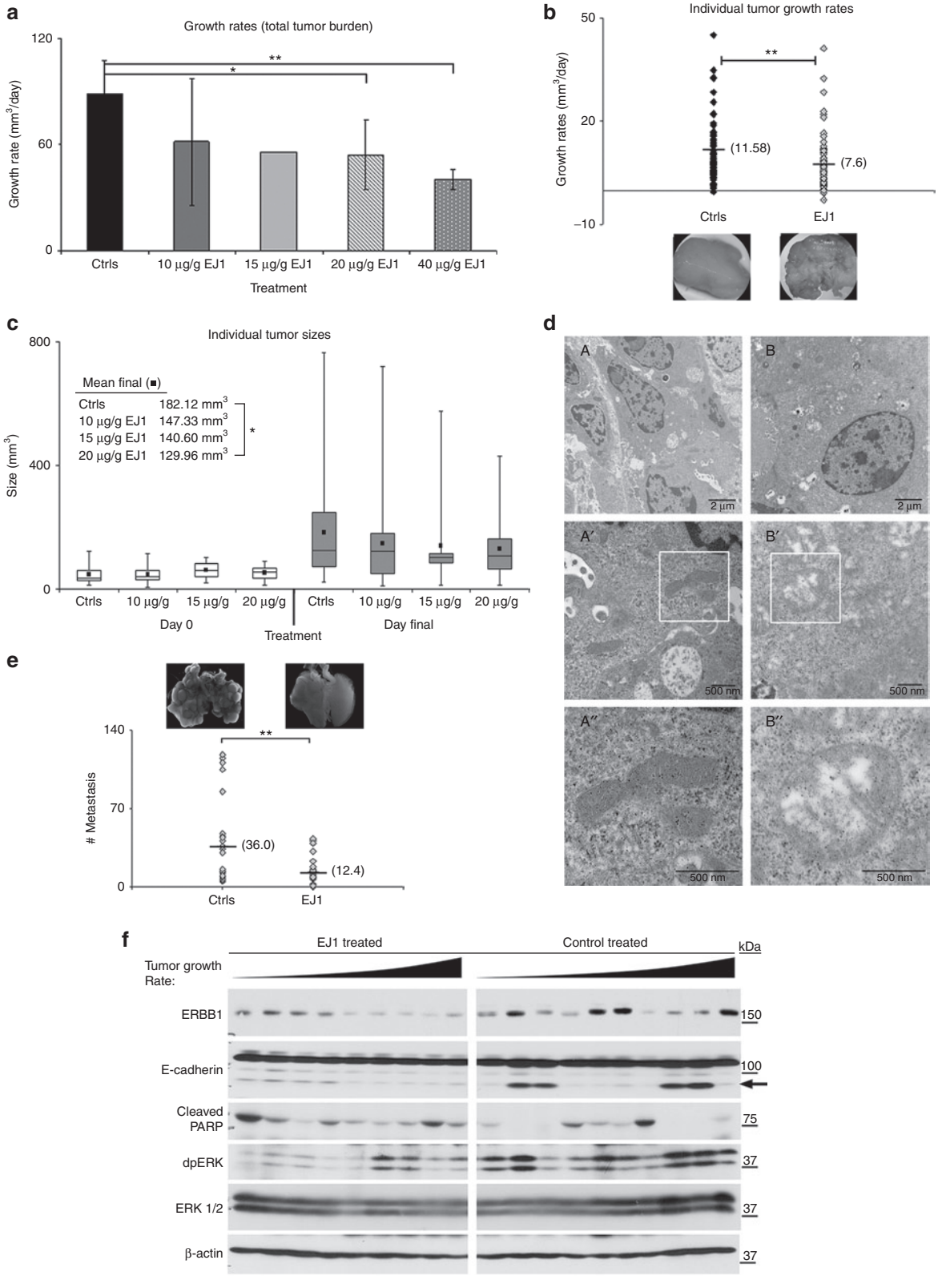

© The American Society of Gene & Cell Therapy

Figure 6 EJ1 peptide inhibits tumor progression in MMTV-pyMT transgenic mice. (**a**) MMTV-PyMT mice were allowed to develop tumors of 50 mm^3 before being treated once daily (i.p. injection) with indicated doses of Ctrls (20 µg/g CP5 (n = 3), PBS (n = 2)) and EJ1 (10 µg/g (n = 6), 15 µg/g (n = 1), and 20 µg/g (n = 7), or twice-daily doses of 40 µg/g (n = 3)). Peaks represent average total tumor burden growth rate in mm^3 per day for each treatment. Error bars, mean ± SD. *P < 0.05; **P < 0.005, Student's t-test. (**b**) Control (12 mice (20 µg/g CP5 (n = 5), PBS (n = 7), n = 100 tumors) vs. 20 µg/g EJ1-treated (eight mice, n =72 tumors) individual tumor growth rates and representative tumor images (insets). Mean denoted by horizontal line. **P < 0.005, Student's t-test. (**c**) Mice were treated with 10, 15, or 20 µg/g body weight EJ1 or control for 21 days and tumors were measured twice weekly. Box plots are shown for day 0 (10 µg/g EJ1: n = 6 mice, 21 tumors; 15 µg/g EJ1: n = 1 mouse, two tumors; 20 µg/g EJ1: n = 8 mice, 24 tumors; Ctrls: n = 12 mice, 41 tumors) and final day (10 µg/g EJ1: n = 6 mice, 46 tumors; 15 µg/g EJ1: n = 1 mouse, nine tumors; 20 µg/g EJ1: n = 8 mice, 72 tumors; Ctrls: n = 12 mice, 100 tumors). Boxes denote median and the second and third quartiles, with whiskers indicating lowest and highest quartiles. Mean values are represented by filled black squares. *P < 0.05, Student's t-test. (**d**) EJ1-(B–B″) and CP (A–A″)-treated tumors from MMTV-PyMT mice were sectioned and imaged by TEM. Representative mitochondria are highlighted in A′–A″ and B′–B″. (**e**) Control vs. EJ1-treated lung tumor numbers. Mean denoted by horizontal line. **P < 0.005, Student's t-test. Representative lung images are also shown. (**f**) Lysates from treated MMTV-pyMT mice (arranged by increasing tumor growth rate) were separated by SDS-PAGE and immunoblotted for the indicated proteins. Arrow indicates 85-kDa E-cadherin species associated with metastasis.[32,33]

We have demonstrated that EJ1 treatment of breast and pancreatic cancer cells possessing wild-type Ras results in a dramatic reduction in the EGF-mediated phosphorylation of ERBB1, ERBB2, and ERBB3, along with reduced cellular viability. Note that in cells with mutant Ras, MDA-MB-231, MIA PaCa-2, and AsPC1, little efficacy was observed, indicating that inactivation of the Ras pathway may be a dominant mechanism for EJ1 activity. Previous studies have shown that the antiparallel dimeric interaction of the helical jxmA (amino acids 645–663) domain is likely important for functional dimerization of the ERBB receptors and for their activation.[13,22,34] Our data suggest that EJ1 could alter dimer activity by altering the structural interaction of endogenous ERBB1/ERBB monomers. The ability of an ERBB1 inhibitor to promote the formation of inactive dimers is not unprecedented. Several groups have demonstrated that the ERBB1 kinase inhibitors AG1478, AG1517, and ZD1839 promote receptor dimerization, while at the same time impairing kinase activity.[35,36] It should be noted, however, that we also visually observed significant receptor clustering in the presence of EJ1 treatment and EGF. Therefore, it is also possible that EJ1 treatment may induce receptor aggregation and that this results in the formation of inactive ERBB multimers.

MLCK-mediated phosphorylation of MLC is one way by which actin cytoskeleton reorganization is regulated and is known to be involved in membrane blebbing.[37,38] In addition, phosphorylation of MLC has been correlated with both cell survival and cell death under different conditions.[39–41] In our system, MLCK and rho kinase (ROCK)-1 inhibitors partially rescued EJ1-induced cell death, indicating an EJ1-mediated induction of MLC phosphorylation was promoting cell death. Alternatively, CaMKII regulates cell cycle progression through activation of Rac1 and increased cyclin D expression.[42,43] We found that EJ1 could effectively downregulate CaMKII activation and that the overexpression of constitutively active Rac1, a downstream effector of CaMKII, could rescue EJ1-induced cell death. This indicates that EJ1 acts on pathways downstream of the ERBBs and CaM to promote MLCK activity and suppress CaMKII activity, resulting in membrane volatility and cell death.

We observed EJ1 accumulation in mitochondria, which was associated with the production of ROS, the loss of MMP, and the formation of swollen or "megamitochondria." These phenomena are known to occur during times of perturbed cellular homeostasis or in response to stressors and are often associated with progression toward apoptosis.[44] It has been shown that although ROS can increase during the early stages of this process, the loss of membrane potential and the resulting mitochondrial swelling ultimately lead to reduced cellular respiration and a reduction in ROS production.[45] It has been suggested that if this process can reduce the levels of ROS to tolerable levels, apoptosis can be avoided, thus serving as an adaptive response to environmental stressors.[44] In cancer cells, where ROS levels can be intrinsically elevated, further increases in ROS levels may be more likely to surpass a critical threshold than in healthy cells and may lead to apoptosis. This difference has been suggested as a possible avenue for cancer therapy.[46] Presumptively, it may relate directly to our study in which we observed mitochondrial swelling but no effect on viability in noncancerous CHO cells. Alternatively, EJ1-induced cell death may require two or more of the mechanisms we have identified, but these additional mechanisms may be lacking in CHO cells. Additionally, it has been demonstrated that an increased intrinsic MMP correlates with increased malignancy, apoptosis resistance, and tumor progression.[47] These insights also suggest possible mechanisms for the preferential targeting of the mitochondria of cancer cells in our animal studies and lack of any overt tissue toxicity.

EJ1 represents a novel pan-ERBB therapeutic agent, targeting multiple activities of the ERBB receptors in a tumor-specific manner, including ERBB activation and downstream CaM-signaling pathways. In addition, EJ1 also targets cells by inducing a reduction of MMP and generation of ROS. Together, these effects result in a highly tumor-specific anticancer therapeutic strategy that may have significant clinical utility.

MATERIALS AND METHODS

Cell culture and plasmids. All cell lines were obtained from the American Type Culture Collection and grown under 5% CO_2. MDA-MB-468, MDA-MB-231, T47D, AsPC1, and BxPC3 cell lines were grown in RPMI (Cellgro) supplemented with 10% (5% for 468 cells) fetal bovine serum. MIA PaCa-2 cells were grown in DMEM and similarly supplemented as per ATCC guidelines. MCF10A cells were grown as previously described.[48] Rac1-WT and Rac1-Q61L plasmids were obtained from Addgene (Cambridge, MA).

Antibodies. The following antibodies were obtained from Santa Cruz Biotechnology (Dallas, TX): EGFR 1005, ERBB3 C-17, and CaMKII. EGFR Ab-13 was obtained from NeoMarkers (Fremont, CA), and the following antibodies were obtained from Cell Signaling (Danvers, MA): p-EGFR (pY845), Her2/ERBB2, Atg12, PARP, cleaved caspase 3, p-ERBB2 (pY1248), p-ERBB3 (pY1289), p-CaMKII (pT286), p-AKT (pS473), AKT, p42/44 MAPK (ERK 1/2), HMGB1, p-p38 (pT180/Y182), and p38. In addition, dpERK and β-actin antibodies were from Sigma (St Louis, MO), E-cadherin antibody was from BD Biosciences (San Jose, CA), and Calmodulin antibody was from Millipore (Billerica, MA).

Peptide synthesis. The EJ peptides were synthesized by GenScript (Scotch Plains, NJ), delivered lyophilized, and stored at −20 °C. Peptides were resuspended as needed at 1 mmol/l in water and stored for up to 2 weeks

© The American Society of Gene & Cell Therapy

at 4 °C. EJ1 peptide sequences are shown conjugated to the PTD4 domain (YARAAARQARA) in **Figure 1c**.

Western blotting, immunoprecipitation, crosslinking/dimerization, and MTT assays. Protein lysate preparation, immunoprecipitation, and western blotting were performed as described previously.[49] For cross-linking, cells were first incubated according to manufacturer instructions with 3 µmol/l DMS, a membrane-permeable, noncleavable, cross-linking agent (Thermo Scientific, Waltham, MA). Cells were analyzed both by the MTT assay following manufacturer's instructions (Sigma) and using a U-Quant Spectrophotometer (Bio-TEK Instruments, Winooski, VT).

Mitochondrial morphology, EJ1 localization, and MMP. Cells were treated with 20 µmol/l CP, 20 µmol/l EJ1 (or FITC-labeled EJ1), and MitoTracker Red CMXRos (Molecular Probes, Carlsbad, CA), along with Hoechst 33342 (Invitrogen, Carlsbad, CA) nuclear stain. Images were taken on an Olympus IX71 and deconvolved using softWoRx 4.0 image analysis software (Applied Precision, Issaquah, WA). Images were brightened using Adobe Photoshop (-Image-Adjustments-Brightness/Contrast). Measurement of MMP was performed with the 5,5′, 6, 6′-tetrachloro-1, 1′, 3, 3′-tetraethyl-benzimidazolcarbocyanine iodide (JC-1) stain (Invitrogen). JC-1 aggregates fluoresce at 590 nm in the mitochondria, whereas cytoplasmically localized JC-1 monomers fluoresce at 529 nm.[50]

Measurement of intracellular ROS by flow cytometry. Generation of intracellular ROS was evaluated by flow cytometry using the 2′,7′-dichlorofluorescein diacetate probe (Invitrogen). Fluorescent cells were analyzed by a FACScan flow cytometer (BD Biosciences) at the Flow Cytometry Shared Service in the Arizona Cancer Center, and the excitation/emission wavelengths were set at 488 and 525 nm, respectively.

Mouse experiments. Tumor studies were performed as described in the study by Bitler *et al.* [49] and **Supplementary Method SM1**, online. The number of metastases in the lungs in MMTV-PyMT mice was assessed in control (six mice) and EJ1-(seven mice) treated mice. Lungs from these mice were fixed, sectioned (10-µm thickness), and stained with hematoxylin and eosin, followed by counting of metastatic foci of five individual sections spanning 200 µm/mouse. A more detailed description of these methods can be found in **Supplementary Method SM1**, online.

SUPPLEMENTARY MATERIAL

Figure S1. Cell line expression of ERBBs and lack of efficacy in CHO and MIA PaCa-2 cells.
Figure S2. EJ1 reduces ERBB1 activation in BxPC3 cells.
Figure S3. EJ1 interacts with EGFR through co-immunoprecipitation.
Figure S4. EGF accumulation at EJ1-induced membrane protrusions.
Figure S5. AG1478 does not cause dynamic changes in membranes of MDA-MB-468 cells.
Figure S6. EJ1 does not induce cell death through autophagy.
Figure S7. EJ1 peptide increases percentage of Annexin V–positive cell populations.
Figure S8. EJ1 induces mitochondrial damage.
Figure S9. Mitochondrial swelling in NIH-3T3, BxPC3, T47D, and CHO cells.
Figure S10. Mitochondrial localization of EJ1 in MDA-MB-468 cells.
Figure S11. EJ1 causes accumulation of reactive oxygen species in MDA-MB-468 cells.
Figure S12. Numbers of MMTV-PyMT tumors and days of study.
Figure S13. Protein expression in the tumors of EJ1 relative to that in control-treated mice.
Figure S14. MMTV–PyMT ERBB2 phosphorylation levels.
Method SM1. Details of the MMTV–PyMT mouse study.

ACKNOWLEDGMENTS

We are grateful to Teresa Horm for insightful comments. This work was supported by funding from the Arizona Biomedical Research Commission (ADHS 13-031230, JAS), the Department of Defense Congressionally Directed Medical Research Commission [W81XWH-11-1-0052 (H-YS) and W81XWH-09-1-0047 (MH)], and the National Cancer Institute (CA023074, CA009213, and CA102113, JAS). The authors have no conflicts of interest to disclose.

REFERENCES

1. Pines, G, Köstler, WJ and Yarden, Y (2010). Oncogenic mutant forms of EGFR: lessons in signal transduction and targets for cancer therapy. *FEBS Lett* **584**: 2699–2706.
2. Zhang, H, Berezov, A, Wang, Q, Zhang, G, Drebin, J, Murali, R *et al.* (2007). ErbB receptors: from oncogenes to targeted cancer therapies. *J Clin Invest* **117**: 2051–2058.
3. Kobayashi, S, Boggon, TJ, Dayaram, T, Jänne, PA, Kocher, O, Meyerson, M *et al.* (2005). EGFR mutation and resistance of non-small-cell lung cancer to gefitinib. *N Engl J Med* **352**: 786–792.
4. Boerner, JL, Demory, ML, Silva, C and Parsons, SJ (2004). Phosphorylation of Y845 on the epidermal growth factor receptor mediates binding to the mitochondrial protein cytochrome c oxidase subunit II. *Mol Cell Biol* **24**: 7059–7071.
5. Coffey, RJ, Hawkey, CJ, Damstrup, L, Graves-Deal, R, Daniel, VC, Dempsey, PJ *et al.* (1997). Epidermal growth factor receptor activation induces nuclear targeting of cyclooxygenase-2, basolateral release of prostaglandins, and mitogenesis in polarizing colon cancer cells. *Proc Natl Acad Sci USA* **94**: 657–662.
6. Demory, ML, Boerner, JL, Davidson, R, Faust, W, Miyake, T, Lee, I *et al.* (2009). Epidermal growth factor receptor translocation to the mitochondria: regulation and effect. *J Biol Chem* **284**: 36592–36604.
7. Lo, HW, Cao, X, Zhu, H and Ali-Osman, F (2010). Cyclooxygenase-2 is a novel transcriptional target of the nuclear EGFR-STAT3 and EGFRvIII-STAT3 signaling axes. *Mol Cancer Res* **8**: 232–245.
8. Wang, YN, Lee, HH, Lee, HJ, Du, Y, Yamaguchi, H and Hung, MC (2012). Membrane-bound trafficking regulates nuclear transport of integral epidermal growth factor receptor (EGFR) and ErbB-2. *J Biol Chem* **287**: 16869–16879.
9. Hsu, SC and Hung, MC (2007). Characterization of a novel tripartite nuclear localization sequence in the EGFR family. *J Biol Chem* **282**: 10432–10440.
10. Liao, HJ and Carpenter, G (2007). Role of the Sec61 translocon in EGF receptor trafficking to the nucleus and gene expression. *Mol Biol Cell* **18**: 1064–1072.
11. Huang, WC, Chen, YJ, Li, LY, Wei, YL, Hsu, SC, Tsai, SL *et al.* (2011). Nuclear translocation of epidermal growth factor receptor by Akt-dependent phosphorylation enhances breast cancer-resistant protein expression in gefitinib-resistant cells. *J Biol Chem* **286**: 20558–20568.
12. Hobert, ME, Kil, SJ, Medof, ME and Carlin, CR (1997). The cytoplasmic juxtamembrane domain of the epidermal growth factor receptor contains a novel autonomous basolateral sorting determinant. *J Biol Chem* **272**: 32901–32909.
13. McLaughlin, S, Smith, SO, Hayman, MJ and Murray, D (2005). An electrostatic engine model for autoinhibition and activation of the epidermal growth factor receptor (EGFR/ErbB) family. *J Gen Physiol* **126**: 41–53.
14. Li, H, Panina, S, Kaur, A, Ruano, MJ, Sánchez-González, P, la Cour, JM *et al.* (2012). Regulation of the ligand-dependent activation of the epidermal growth factor receptor by calmodulin. *J Biol Chem* **287**: 3273–3281.
15. Li, H and Villalobo, A (2002). Evidence for the direct interaction between calmodulin and the human epidermal growth factor receptor. *Biochem J* **362**(Pt 2): 499–505.
16. Sengupta, P, Bosis, E, Nachliel, E, Gutman, M, Smith, SO, Mihályné, G *et al.* (2009). EGFR juxtamembrane domain, membranes, and calmodulin: kinetics of their interaction. *Biophys J* **96**: 4887–4895.
17. Wada, T, Qian, XL and Greene, MI (1990). Intermolecular association of the p185neu protein and EGF receptor modulates EGF receptor function. *Cell* **61**: 1339–1347.
18. Goldman, R, Levy, RB, Peles, E and Yarden, Y (1990). Heterodimerization of the erbB-1 and erbB-2 receptors in human breast carcinoma cells: a mechanism for receptor transregulation. *Biochemistry* **29**: 11024–11028.
19. Li, H, Sánchez-Torres, J, Del Carpio, A, Salas, V and Villalobo, A (2004). The ErbB2/Neu/HER2 receptor is a new calmodulin-binding protein. *Biochem J* **381**(Pt 1): 257–266.
20. Li, H, Ruano, MJ and Villalobo, A (2004). Endogenous calmodulin interacts with the epidermal growth factor receptor in living cells. *FEBS Lett* **559**: 175–180.
21. Chen, QQ, Chen, XY, Jiang, YY and Liu, J (2005). Identification of novel nuclear localization signal within the ErbB-2 protein. *Cell Res* **15**: 504–510.
22. Jura, N, Endres, NF, Engel, K, Deindl, S, Das, R, Lamers, MH *et al.* (2009). Mechanism for activation of the EGF receptor catalytic domain by the juxtamembrane segment. *Cell* **137**: 1293–1307.
23. Dillon, C, Creer, A, Kerr, K, Kümin, A and Dickson, C (2002). Basolateral targeting of ERBB2 is dependent on a novel bipartite juxtamembrane sorting signal but independent of the C-terminal ERBIN-binding domain. *Mol Cell Biol* **22**: 6553–6563.
24. Ho, A, Schwarze, SR, Mermelstein, SJ, Waksman, G and Dowdy, SF (2001). Synthetic protein transduction domains: enhanced transduction potential *in vitro* and in vivo. *Cancer Res* **61**: 474–477.
25. Martín-Nieto, J and Villalobo, A (1998). The human epidermal growth factor receptor contains a juxtamembrane calmodulin-binding site. *Biochemistry* **37**: 227–236.
26. Clapham, DE (2007). Calcium signaling. *Cell* **131**: 1047–1058.
27. Yuan, K, Chung, LW, Siegal, GP and Zayzafoon, M (2007). alpha-CaMKII controls the growth of human osteosarcoma by regulating cell cycle progression. *Lab Invest* **87**: 938–950.
28. Scaffidi, P, Misteli, T and Bianchi, ME (2002). Release of chromatin protein HMGB1 by necrotic cells triggers inflammation. *Nature* **418**: 191–195.
29. Kroemer, G, Galluzzi, L and Brenner, C (2007). Mitochondrial membrane permeabilization in cell death. *Physiol Rev* **87**: 99–163.
30. Maglione, JE, Moghanaki, D, Young, LJ, Manner, CK, Ellies, LG, Joseph, SO *et al.* (2001). Transgenic Polyoma middle-T mice model premalignant mammary disease. *Cancer Res* **61**: 8298–8305.

© The American Society of Gene & Cell Therapy

31. Guy, CT, Cardiff, RD and Muller, WJ (1992). Induction of mammary tumors by expression of polyomavirus middle T oncogene: a transgenic mouse model for metastatic disease. *Mol Cell Biol* **12**: 954–961.
32. Kuefer, R, Hofer, MD, Gschwend, JE, Pienta, KJ, Sanda, MG, Chinnaiyan, AM *et al.* (2003). The role of an 80 kDa fragment of E-cadherin in the metastatic progression of prostate cancer. *Clin Cancer Res* **9**: 6447–6452.
33. Grabowska, MM, Sandhu, B and Day, ML (2012). EGF promotes the shedding of soluble E-cadherin in an ADAM10-dependent manner in prostate epithelial cells. *Cell Signal* **24**: 532–538.
34. Hubbard, SR (2009). The juxtamembrane region of EGFR takes center stage. *Cell* **137**: 1181–1183.
35. Arteaga, CL, Ramsey, TT, Shawver, LK and Guyer, CA (1997). Unliganded epidermal growth factor receptor dimerization induced by direct interaction of quinazolines with the ATP binding site. *J Biol Chem* **272**: 23247–23254.
36. Anido, J, Matar, P, Albanell, J, Guzmán, M, Rojo, F, Arribas, J *et al.* (2003). ZD1839, a specific epidermal growth factor receptor (EGFR) tyrosine kinase inhibitor, induces the formation of inactive EGFR/HER2 and EGFR/HER3 heterodimers and prevents heregulin signaling in HER2-overexpressing breast cancer cells. *Clin Cancer Res* **9**: 1274–1283.
37. Holzapfel, G, Wehland, J and Weber, K (1983). Calcium control of actin-myosin based contraction in triton models of mouse 3T3 fibroblasts is mediated by the myosin light chain kinase (MLCK)-calmodulin complex. *Exp Cell Res* **148**: 117–126.
38. Mills, JC, Stone, NL, Erhardt, J and Pittman, RN (1998). Apoptotic membrane blebbing is regulated by myosin light chain phosphorylation. *J Cell Biol* **140**: 627–636.
39. Connell, LE and Helfman, DM (2006). Myosin light chain kinase plays a role in the regulation of epithelial cell survival. *J Cell Sci* **119**(Pt 11): 2269–2281.
40. Fazal, F, Gu, L, Ihnatovych, I, Han, Y, Hu, W, Antic, N *et al.* (2005). Inhibiting myosin light chain kinase induces apoptosis *in vitro* and in vivo. *Mol Cell Biol* **25**: 6259–6266.
41. Jin, Y, Atkinson, SJ, Marrs, JA and Gallagher, PJ (2001). Myosin ii light chain phosphorylation regulates membrane localization and apoptotic signaling of tumor necrosis factor receptor-1. *J Biol Chem* **276**: 30342–30349.
42. Fleming, IN, Elliott, CM, Buchanan, FG, Downes, CP and Exton, JH (1999). Ca2+/calmodulin-dependent protein kinase II regulates Tiam1 by reversible protein phosphorylation. *J Biol Chem* **274**: 12753–12758.
43. Buchanan, FG, Elliot, CM, Gibbs, M and Exton, JH (2000). Translocation of the Rac1 guanine nucleotide exchange factor Tiam1 induced by platelet-derived growth factor and lysophosphatidic acid. *J Biol Chem* **275**: 9742–9748.
44. Wakabayashi, T (2002). Megamitochondria formation - physiology and pathology. *J Cell Mol Med* **6**: 497–538.
45. Teranishi, M, Karbowski, M, Kurono, C, Soji, T and Wakabayashi, T (1999). Two types of the enlargement of mitochondria related to apoptosis: simple swelling and the formation of megamitochondria. *J Electron Microsc (Tokyo)* **48**: 637–651.
46. Trachootham, D, Alexandre, J and Huang, P (2009). Targeting cancer cells by ROS-mediated mechanisms: a radical therapeutic approach? *Nat Rev Drug Discov* **8**: 579–591.
47. Gogvadze, V (2011). Targeting mitochondria in fighting cancer. *Curr Pharm Des* **17**: 4034–4046.
48. Bitler, BG, Goverdhan, A and Schroeder, JA (2010). MUC1 regulates nuclear localization and function of the epidermal growth factor receptor. *J Cell Sci* **123**(Pt 10): 1716–1723.
49. Bitler, BG, Menzl, I, Huerta, CL, Sands, B, Knowlton, W, Chang, A *et al.* (2009). Intracellular MUC1 peptides inhibit cancer progression. *Clin Cancer Res* **15**: 100–109.
50. Salvioli, S, Ardizzoni, A, Franceschi, C and Cossarizza, A (1997). JC-1, but not DiOC6(3) or rhodamine 123, is a reliable fluorescent probe to assess delta psi changes in intact cells: implications for studies on mitochondrial functionality during apoptosis. *FEBS Lett* **411**: 77–82.